High Pressure Research
An International Journal

ISSN: 0895-7959 (Print) 1477-2299 (Online) Journal homepage: http://www.tandfonline.com/loi/ghpr20

Studying the effect of hydrogen on diamond growth by adding $C_{10}H_{10}Fe$ under high pressures and high temperatures

Chao Fang, Xiaopeng Jia, Shishuai Sun, Bingmin Yan, Yadong Li, Ning Chen, Yong Li & Hong-an Ma

To cite this article: Chao Fang, Xiaopeng Jia, Shishuai Sun, Bingmin Yan, Yadong Li, Ning Chen, Yong Li & Hong-an Ma (2016) Studying the effect of hydrogen on diamond growth by adding $C_{10}H_{10}Fe$ under high pressures and high temperatures, High Pressure Research, 36:1, 42-54, DOI: 10.1080/08957959.2015.1129405

To link to this article: http://dx.doi.org/10.1080/08957959.2015.1129405

HIGH PRESSURE RESEARCH, 2016
VOL. 36, NO. 1, 42–54
http://dx.doi.org/10.1080/08957959.2015.1129405

Taylor & Francis
Taylor & Francis Group

Studying the effect of hydrogen on diamond growth by adding $C_{10}H_{10}Fe$ under high pressures and high temperatures

Chao Fang[a], Xiaopeng Jia[a], Shishuai Sun[b], Bingmin Yan[c], Yadong Li[a], Ning Chen[a], Yong Li[d] and Hong-an Ma[a]

[a]State Key Laboratory of Superhard Materials, Jilin University, Changchun, People's Republic of China;; [b]College of Science, Tianjin University of Technology, Tianjin, People's Republic of China; [c]Center for High Pressure Science & Technology Advanced Research, Changchun, People's Republic of China; [d]Physical and Applied Engineering Department, Tongren University, Tongren, People's Republic of China

ABSTRACT

In this paper, hydrogen-doped industrial diamonds and gem diamonds were synthesized in the Fe–Ni–C system with $C_{10}H_{10}Fe$ additive, high pressures and high temperatures range of 5.2–6.2 GPa and 1250–1460°C. Experimental results indicate similar effect of hydrogen on these two types of diamonds: with the increasing content of $C_{10}H_{10}Fe$ added in diamond growth environment, temperature is a crucial factor that sensitively affects the hydrogen-doped diamond crystallization. The temperature region for high-quality diamond growth becomes higher and the morphology of diamond crystal changes from cube-octahedral to octahedral. The defects on the {100} surfaces of diamond are more than those on the {111} surfaces. Fourier transform infrared spectroscopy (FTIR) results indicate that the hydrogen atoms enter into the diamond crystal lattice from {100} faces more easily. Most interestingly, under low temperature, nitrogen atoms can also easily enter into the diamond crystal lattice from {100} faces cooperated with hydrogen atoms.

ARTICLE HISTORY
Received 16 November 2015
Accepted 4 December 2015

KEYWORDS
diamond; HPHT; hydrogen-doped; $C_{10}H_{10}Fe$

1. Introduction

Diamond is an exclusive material for mechanical and electronic applications because of its exceptional physical and chemical properties.[1–3] Various approaches have been developed to fabricate high-performance diamond-based devices by engineering their bandgaps so as to improve their semiconducting properties. One of the most feasible methods to control the semiconducting properties of diamond is doping the carbon with hetero atoms such as nitrogen, boron.[4–8] In addition to the nitrogen and boron, experimental studies and theoretical calculations have indicated that the hydrogen-related defects present in the structure of diamond are of fundamental importance.[9–11] Meanwhile, hydrogen is also a dominant impurity in most natural diamonds and the latest study found large amounts of hydrogen exist in the mantle.[12] So there must be a lot of hydrogen in natural diamond growth environment. Unfortunately, its behavior doping into diamonds is still unclear. Therefore, the development and synthesis of

CONTACT Hong-an Ma ✉ maha@jlu.edu.cn

hydrogen-doped diamond, especially the gem-diamond, are important for further understanding the effects of hydrogen doping on diamond and provide some important information for the genesis of natural diamond.

Previously, the field of hydrogen-doped diamond films has been studied with respect to structure, growth rate, and electrical properties.[13–15] It is widely reported that hydrogen is a key component of the gas mixture usually used for diamond nucleation and growth by chemical vapour deposition (CVD) methods.[16] However, most diamond films made by CVD method are polycrystalline, and hydrogen is readily positioned at CVD diamond films in grain boundary region as well as on the crystallite surface. These structural flaws greatly degrade the properties of diamond films. Recent advances in the synthesis of single-crystal diamond via high pressures and high temperatures (HPHT) have demonstrated that material with exceptional electronic and optical properties can now be produced, and this has enlivened interest in exploiting the extraordinary properties of diamond.[17,18] Therefore, the development and synthesis of hydrogen-doped diamonds under HPHT conditions are important for their promising applications in many fields. Available literature data clearly show that hydrogen plays a significant role in the synthetic process of diamond at high pressure.[19,20] Although the hydrogen-doped diamond single crystal has been synthesized under HPHT conditions with LiH and TiH_2 additive,[21,22] the presence of Li and Ti impurities will certainly influence the general features and peculiarities of diamond crystallization in the presence of hydrogen. In our group earlier work, we have successfully synthesized the diamonds only doped with hydrogen by the film growth method (FGM).[23] However, experimental studies on diamond crystallization and the growth of large gem-diamond in the presence of hydrogen at HPHT conditions are quite limited. What is more, high-quality large hydrogen-doped diamonds can be widely used in many fields and are more proper to be used study the effect of hydrogen doping. So, more detailed information about the effect of hydrogen impurity on diamond growth by HPHT synthesis is an essential prerequisite for understanding the influence of hydrogen on electrical and optical properties, and ultimately exploiting the full potential of these materials. There remains a deeper understanding for investigating the effect of hydrogen doping into diamond crystal under HPHT.

With respect to this, we have synthesized industrial diamonds and gem-diamond single crystals by FGM and temperature gradient method (TGM), respectively. The effect of hydrogen on diamond growth by HPHT became more clearly, and these results will provide some important information for the synthesis of hydrogen-doped diamond and the genesis of natural diamond.

2. Experimental details

Experiments on diamond crystallization were carried out using a china-type large volume Cubic High Pressure Apparatus (SPD-6 × 1200). The design of the apparatus and scheme of high pressure cell for diamond crystallization is shown in Figure 1. Diamonds were synthesized through FGM in Figure 1(a) and TGM in Figure 1(b). The starting materials were the high-purity graphite powers (99. 99% purity) as carbon sources. The Fe–Ni alloy powders (200 mesh) and sheet were used as the solvent catalysts for FGM and TGM, respectively. In order to obviously investigate the effect of hydrogen element on diamond growth, we choose ferrocene ($C_{10}H_{10}Fe$) powders as additional component in

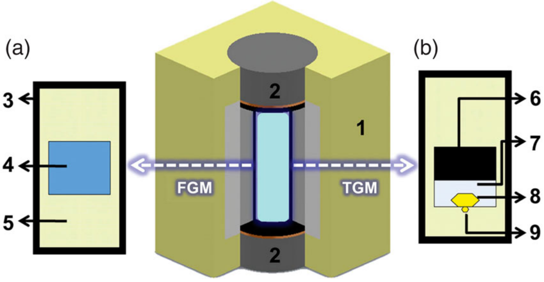

Figure 1. Sample assembly for diamond synthesized by HPHT: 1. pyrophyllite; 2. conductive steel ring; 3. graphite heater; 4. cavity; 5. insulator; 6. carbon source; 7. alloy catalyst; 8. as-grown diamond; 9. seed crystal.

the range of 0–0.3 wt% (weight ratio in catalysts). Due to the decomposition of ferrocene at high temperature (>500°C), the major impurity in the synthetic chamber is the hydrogen element.[23] High-quality seed crystals with {111} facets were selected as the growth facet for TGM. For FGM, firstly we sufficiently mixed the powder of $C_{10}H_{10}Fe$, graphite and Fe–Ni alloy for 4 h. Then the mixed powder was pre-pressed to a sample disk. Each of the sample assembly was dried by heating to 120°C for 2 h before being placed in the high pressure apparatus to remove the influence of the residual water on the growth of diamonds. The synthetic conditions were 5.2–6.2 GPa and 1250–1460°C. The pressure was calibrated by the pressure-induced phase transitions of bismuth, thallium, and barium. The temperature was measured by the Pt6%Rh–Pt30%RH thermocouple, whose junction was placed near the crystallization sample.

After the HPHT experiments, the collected samples were placed in a bottle of a boiling mixture of H_2SO_4 and HNO_3 to remove the metal catalysts and graphite powders. The morphology and color of the synthesized diamonds were characterized by optical microscopy and scanning electron microscope (SEM). The chemical composition and atomic-level hybrid qualities information of impurity doped into diamonds were confirmed by the Fourier transform infrared (FTIR) spectrometry and Raman spectrometry.

3. Results and discussion

3.1. The effect on synthetic conditions with additive $C_{10}H_{10}Fe$

The main parameters of the obtained diamonds are summarized in Table 1. The experiments (N-(1-7)) were run at synthetic pressure 5.2–5.4 GPa and temperature 1250–1460°C by FGM. In experiments performed at 5.2 GPa, the diamond nucleation and growth are established in the Fe–Ni–C system, the synthesized diamonds are yellow in color, and exhibit cubic, cub-octahedral, and octahedral shape at 1250°C, 1350°C, and 1400°C (N-1), respectively. The average size is about 0.2–0.3 mm in a 15 min run (Figure 2(a)). When the $C_{10}H_{10}Fe$ are added into the Fe–Ni–C system, the diamond growth habits change. In run N-2, the diamond nucleation growth is established with temperature increasing up to 1270°C. However, we notice from Figure 2(b) that the obtained diamonds exhibit cubic shape with light green color and some linear inclusions. The morphology of the synthesized diamond crystals vary from cubic, cubic-octahedral to octahedral shape

Table 1. The corresponding experimental parameters of diamond synthesize with $C_{10}H_{10}Fe$ additive under HPHT conditions.

Run	$C_{10}H_{10}Fe$ (wt.%)	Pressure (GPa)	Temperature (°C)	Morphology	Color	Size (mm)	Method
N-1	0	5.2	1250–1400	{100}and{111}	Yellow	0.2–0.3	FGM
N-2	0.1	5.3	1270–1320	{100}	Light green	0.15–0.2	FGM
N-3	0.1	5.3	1320–1360	{100}and{111}	Greenish yellow	0.15–0.2	FGM
N-4	0.1	5.3	1360–1440	{111}	Yellow	0.15–0.2	FGM
N-5	0.2	5.4	1300–1330	{100}	Black	0.16–0.22	FGM
N-6	0.2	5.4	1330–1370	{100}and{111}	Black	0.16–0.22	FGM
N-7	0.2	5.4	1370–1460	{111}	Greenish yellow	0.16–0.22	FGM
N-8	0	5.7	1280–1320	{100}and{111}	Yellow	2.1–2.5	TGM
N-9	0.1	5.9	1320–1350	{100}and{111}	Yellow	2.2–2.6	TGM
N-10	0.3	6.2	1360–1380	{100}and{111}	Yellow	2.9–3.2	TGM
N-11	0.3	6.2	1390–1450	{111}	Yellow	3.2–3.5	TGM

with the increase in temperature at 5.3 GPa (N-3 and 4) and the color of these diamonds change from greenish yellow to yellow (Figure 2(c)–(d)). The growth habits and color for the synthesized diamonds significantly change with the 0.2 wt% $C_{10}H_{10}Fe$ additive in the Fe–Ni–C system (N-(5-7)). The quality of crystals becomes poor, and the crystals tend to be black at 5.4 GPa, 1300–1370°C (Figure 3(a) and 3(b)). At higher temperatures of 1370–1460°C (N-7), the obtained diamonds with octahedron shape are greenish yellow, transparent, and nearly do not contain any inclusions (Figure 3(c)). These results indicate that temperature is a crucial factor that sensitively affects the diamond crystallization in the Fe–Ni–C system with $C_{10}H_{10}Fe$ additive by FGM. To obtained high-quality hydrogen-doped diamond crystal, the appropriate temperature is necessary.

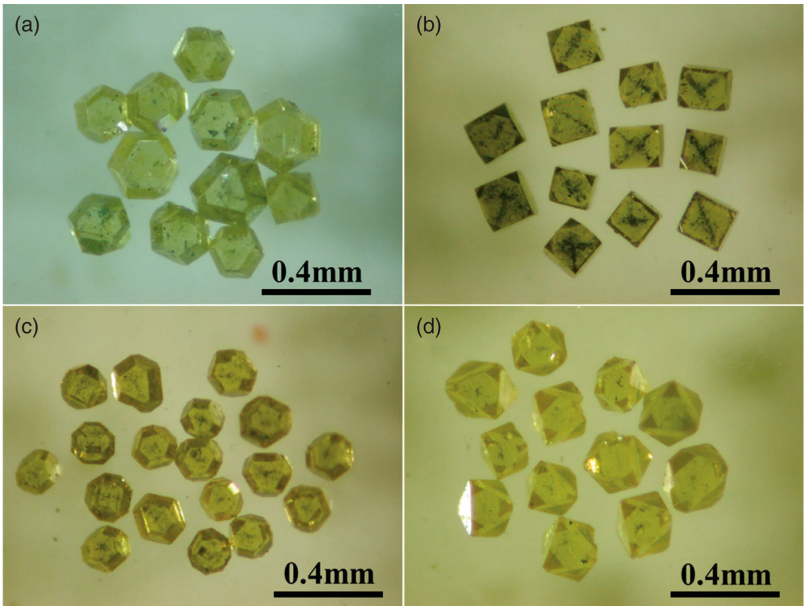

Figure 2. Optical image of the diamond crystals synthesized from the Fe–Ni–C system by FGM: (a) conventional Fe–Ni–C system and (b)–(d) with 0.1 wt% $C_{10}H_{10}Fe$ additive at 1270°C, 1320°C, 1360°C, respectively.

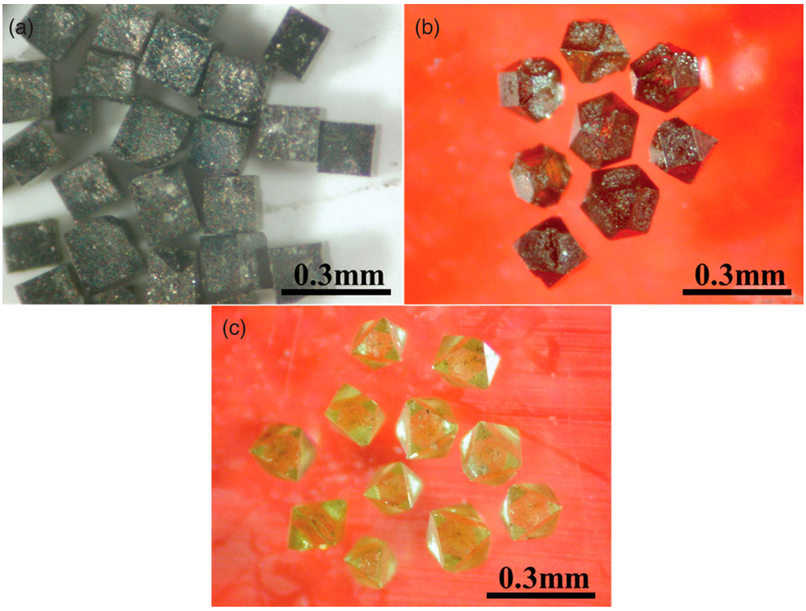

Figure 3. Optical image of the diamond crystals synthesized from the Fe–Ni–C system with 0.2 wt% $C_{10}H_{10}Fe$ addition by FGM at: (a) 1300°C, (b) 1330°C and (c) 1370°C, respectively.

The experiments (N-(8-11)) are run at 5.7–6.2 GPa, 1280–1450°C by TGM. A reference experiment (N-8) is performed without hydrogen additives. The crystal (Figure 4(a)) has a cub-octahedral habit and exhibits {111} and {100} faces. All the surfaces are flat. The diamond synthesized at 5.9 GPa (N-9) is cub-octahedral and exhibits {111} and {100} faces at 1330°C with 0.1 wt% $C_{10}H_{10}Fe$ additive (Figure 4(b)). When increasing the $C_{10}H_{10}Fe$ addition to 0.3 wt%, the diamonds were synthesized at pressure 6.2 GPa and temperature 1370°C (N-10), 1420°C (N-11), respectively. For the crystal grown at lower temperature 1370°C, in Figure 4(c), it is found that there are plenty of pits and some linear inclusions on the {100} face. However, the {111} surface has little pits and almost flat. When increasing temperatures to 1420°C, all surfaces of the obtained diamond with octahedron shape are flat and nearly do not contain any inclusions (Figure 4(d)). These results are in good agreement with the above results by FGM: when the concentration of hydrogen is constant in the growth environment, improving appropriate temperature can help in obtaining a high-quality hydrogen-doped diamond.

Meanwhile we also noticed that the pressure for diamond crystallization increases about 0.2 and 0.5 GPa by FGM and TGM, respectively. We believe these results can be explained as follows. For different catalysts, the metal–diamond eutectic lines are different. When the $C_{10}H_{10}Fe$ additive was added into the reaction system, a great deal of H decomposed from the $C_{10}H_{10}Fe$. Hydrogen will bring about changes in the characteristics of catalysts, such as melting point, glutinosity, the liquid surface tension, the capability of dissolving graphite, etc. which leads to higher synthesis conditions (pressure and temperature) of diamond crystallization.

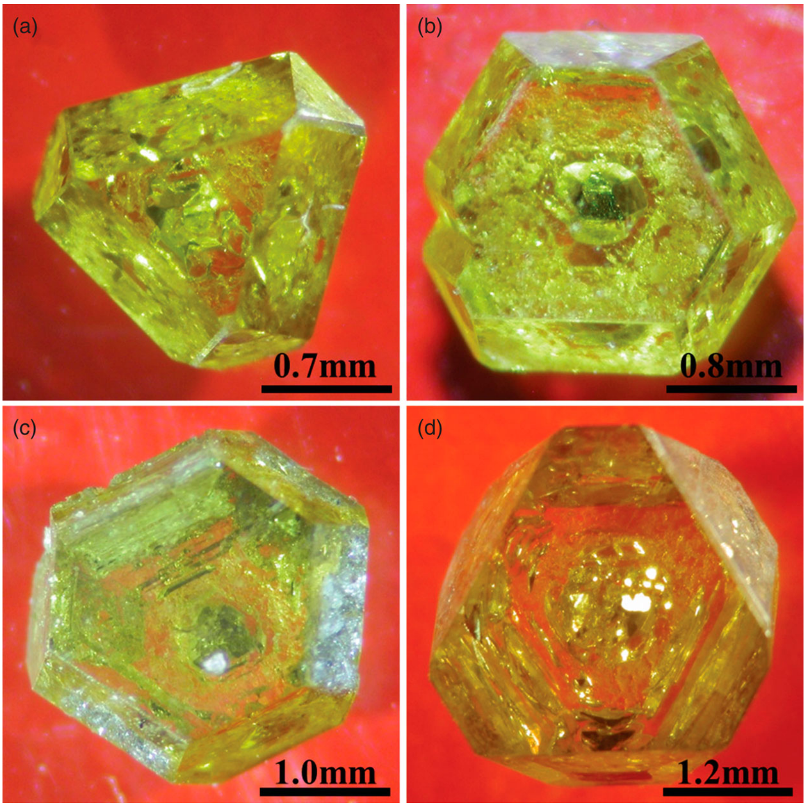

Figure 4. Optical image of the diamond crystals synthesized from the Fe–Ni–C system by TGM at: (a) conventional Fe–Ni–C system, (b) with 0.1 wt.% $C_{10}H_{10}Fe$ additive and (c, d) with 0.3 wt% $C_{10}H_{10}Fe$ additive at 1360°C, 1420°C, respectively.

3.2. The different effects on morphology of {100} and {111} faces with additive $C_{10}H_{10}Fe$

SEM photographs were recorded to further carefully analyze the surface configuration of the synthesized diamond. Figures 5 and 6 correspond to the results of diamonds synthesized by FGM and TGM, respectively. Figure 5(a) shows that the diamond synthesized in the Fe–Ni–C system with 0.2 wt% $C_{10}H_{10}Fe$ additive is predominantly composed of the {100} faces and the surfaces look very rough. It is observed from Figure 5(b) that the numerous depressions are presented on the {100} surfaces. Although some depression defects are still observed on the {111} faces (Figure 5(c)–(d)), the number of depression decreases in contrast to the {100} surface of the synthesized diamond. Figure 6(a) and 6 (b) shows the diamonds synthesized in the conventional Fe–Ni–C system by TGM. It is found that both {100} and {111} faces are flat. It is interesting to note from Figure 6(c) and 6(d) that plenty of rough defects are found on the {100} faces, whereas the {111} faces are still flat in the Fe–Ni–C system with 0.3 wt% $C_{10}H_{10}Fe$ additive. The main reasons for the phenomenon can be analyzed as the following: first, it is generally believed that the surface patterns are related to the use of solvent metal in the diamond growth process.[24] The different solvent metals will bring about the change of the diamond

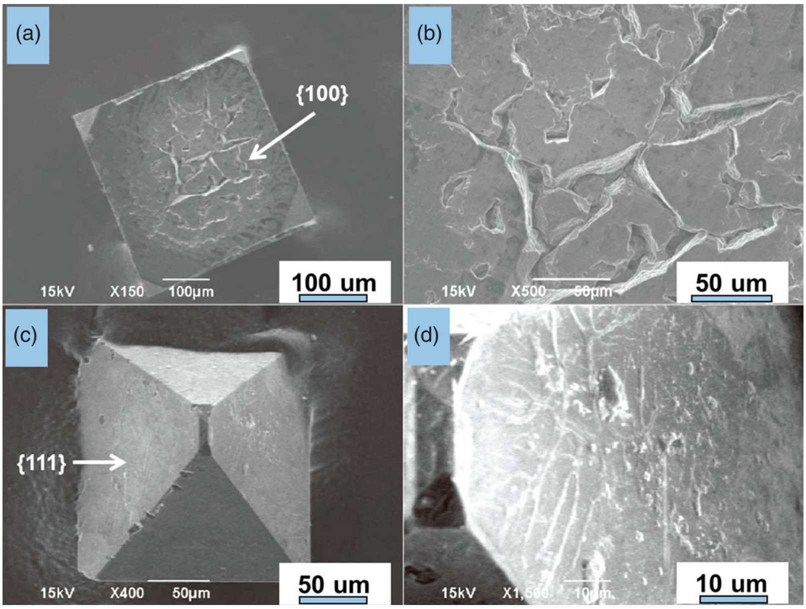

Figure 5. SEM images of the diamond crystal grown from the Fe–Ni–C system with 0.2 wt% $C_{10}H_{10}Fe$ additive by FGM: (a, b) cubic shape with {100} faces and the partial enlarged drawing and (c, d) octahedral shape with {111} faces and the partial enlarged drawing.

surface patterns. When the hydrogen atoms were mixed in the diamond growth environment, the characteristics of epitaxial crystallization of solvent metals were changed with different degrees, resulting in different patterns on the diamond surfaces.[23] Second, the atoms on the {100} and {111} surfaces have two and one unsaturated bonds,

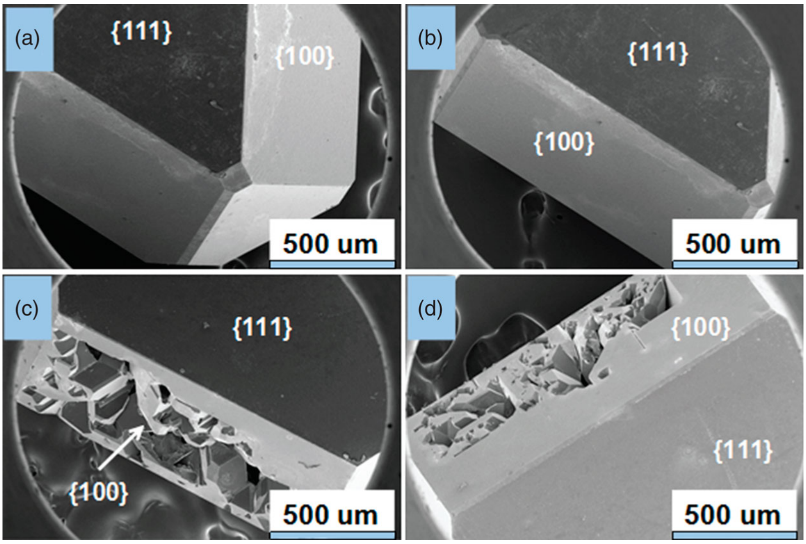

Figure 6. SEM images of the diamond crystal grown from the Fe–Ni–C system by TGM: (a)–(b) conventional Fe–Ni–C system and (c)–(d) with 0.3 wt% $C_{10}H_{10}Fe$ additive.

respectively. Thus, it leads to the different adsorption capacities for the {100} and {111} faces. The {111} surface should be more steady than {100}, thus the {111} surface is more difficult to be etched by hydrogen. So, the patterns on the {100} surfaces of diamond with hydrogen additive are different from the {111} surface.

3.3. The effect on impurities and defect species in diamond with additive $C_{10}H_{10}Fe$

Infrared absorption spectroscopy is extremely useful for identifying impurities and defect species in diamond. A number of diamond crystals of suitable quality synthesized at different *P*–*T* conditions were selected for the infrared absorption measurements. Figure 7 is the typical FTIR recorded for the synthesized diamond crystals by FGM. It can be seen that with decreasing growth temperature the absorption peak exhibits a number of systematic changes. The hydrogen-related absorption is hardly found in the diamond (Figure 7(a)) without any $C_{10}H_{10}Fe$ additive. However, when 0.1 wt% $C_{10}H_{10}Fe$ is added, two absorption peaks located at around 2850 cm^{-1} (sp^3–CH_3) and 2920 cm^{-1} (sp^3–CH_2–) indicate that hydrogen is incorporated into diamond lattice, as exhibited in Figures 7(b)–(d).[25,26] Additionally, the tendency shown clearly in Figures 7(b)–(d) is that the intensities of the 2850 and 2920 cm^{-1} hydrogen-related peaks increase with the decrease in temperature. This result shows that the hydrogen can more easily be incorporated into the diamond accompanying with the formation of {100} faces at low temperature. In addition, the absorption intensities in the defect-induced one-phonon region from 1000 to 1350 cm^{-1} caused by nitrogen impurity change significantly. The IR reveals that the synthesized diamond crystals contain nitrogen impurity in the form of C-center with a single substitutional nitrogen atom. The nitrogen impurity concentration can be evaluated according to the absorption coefficient of IR spectra, determined by the formula as follows:[27,28]

$$\mathrm{Nc(ppm)} = \mu(1130\ \mathrm{cm}^{-1})/\mu(2120\ \mathrm{cm}^{-1}) \times 5.5 \times 25,$$

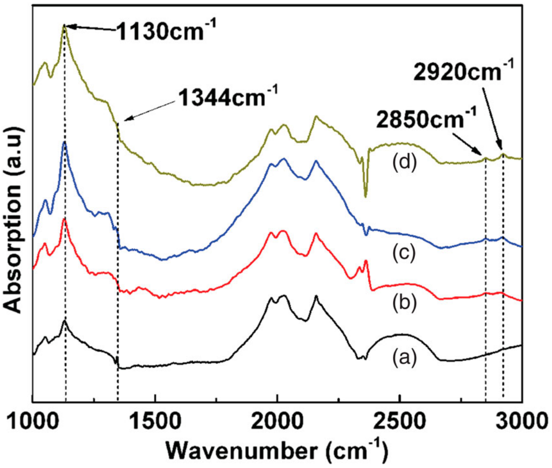

Figure 7. (Colour online) The typical FTIR recorded for the synthesized diamond crystals by FGM: (a) conventional Fe–Ni–C system and (b)–(d) with 0.1 wt% $C_{10}H_{10}Fe$ additive at 1360°C, 1320°C, 1270°C, respectively.

Table 2. Nitrogen concentrations in diamonds synthesized with 0.1 wt.% $C_{10}H_{10}Fe$ additive corresponding to the Figure 7.

Sample	Nitrogen concentration (ppm)
A	350
B	400
C	630
D	800

where Nc (ppm) is the concentration of nitrogen, μ (1130 cm^{-1}) and μ (2120 cm^{-1}) represent the absorption intensity of 1130 cm^{-1} and dip at 2120 cm^{-1}, respectively. Based on the intensity of the peak in Figure 7(a), the nitrogen concentration of diamond synthesis in the Fe–Ni–C system was evaluated as 300–350 ppm according to the above formula. However, the substitutional nitrogen concentration in diamond increases from 400 to 800 ppm with decreasing temperature (Table 2), which is the same as the change of hydrogen in diamond. Based on the FGM of diamond growth, as the temperature is lower, the diamond growth rate was faster at the same pressure, so the impurity would be easier to incorporate into the structure of diamond crystal, which may be one of the reasons for the above phenomenon. Another reason may be that appropriate amount of hydrogen additive contributes to the incorporation of nitrogen into the structure of diamond according to the previous report.[23]

Figure 8 is the typical FTIR recorded for the synthesized gem-diamond single crystals by TGM. We can see that the hydrogen-related absorption is hardly found in the diamond (Figure 8(a)) without any $C_{10}H_{10}Fe$ additive. However, three absorption peaks located at around 2850, 2920 and 2960 cm^{-1} (C–H)[29] appear (Figure 8(b) and 8(c)) and the intensities of these hydrogen-related peaks increase (inset image lying at top right corners) with increasing the addition of $C_{10}H_{10}Fe$. These results indicate that the hydrogen was successfully doped into the gem-diamond.

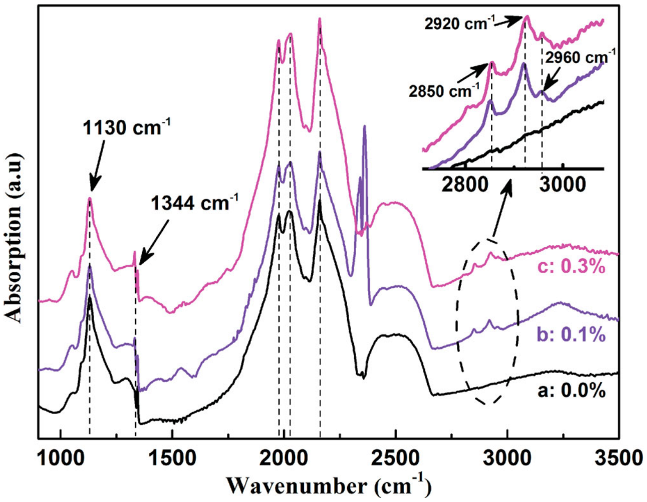

Figure 8. (Colour online) The typical FTIR recorded of the diamond crystals synthesized from the Fe–Ni–C system with $C_{10}H_{10}Fe$ additive by TGM: (a) 0.0 wt.%, (b) 0.1 wt.% and (c) 0.3 wt.%.

In order to capture more detailed information on the effect of hydrogen impurity on the growth process of HPHT synthesis gem-diamond, the IR of {100} and {111} faces in the same diamond synthesized with 0.3 wt% $C_{10}H_{10}Fe$ addition is shown in Figure 9. The curve (a) in Figure 9 shows the IR of {111} crystal face grown at higher temperature region, and the strength of nitrogen-related (1130 and 1344 cm^{-1}) and hydrogen-related (2850, 2920 and 2960 cm^{-1}) absorptions are weak. Nevertheless, {100} crystal face grown at lower temperature region shows significantly different infrared spectrum (curve b in Figure 9). It is interesting that the strength of nitrogen-related and hydrogen-related (inset image lying at top right corner) absorptions of diamond becomes stronger. These results also are in good agreement with the above IR results of industrial diamonds. So, under low temperature, nitrogen atoms can also easily enter into the diamond crystal lattice from {100} face cooperated with hydrogen atoms.

3.4. The effect on the chemical bonds of graphite carbons with additive $C_{10}H_{10}Fe$

Raman spectroscopy is an ideal tool for the investigation of carbon compounds, since their Raman spectra have been found to respond to changes in the microscopic structure of the crystals. In this study, Raman spectroscopy has been used to study the effect of additive $C_{10}H_{10}Fe$ on the chemical bonds of graphite carbons. The typical Raman spectrum for these black crystals (Run N-5) is shown in Figure 10. A sharp peak at 1331.94 cm^{-1} is observed, which is a diamond peak with C–C sp^3 bonds. The other very noticeable Raman peak is ~2078 cm^{-1}, which is not the base frequency of some radical and double frequency or the combined frequency of ~1331.23 cm^{-1} and (or) other peaks. We notice the wavenumber of graphite at 1580 cm^{-1} is shifted to 1544 cm^{-1}. The presence of graphite in the synthesized diamond is the main reason that the color of

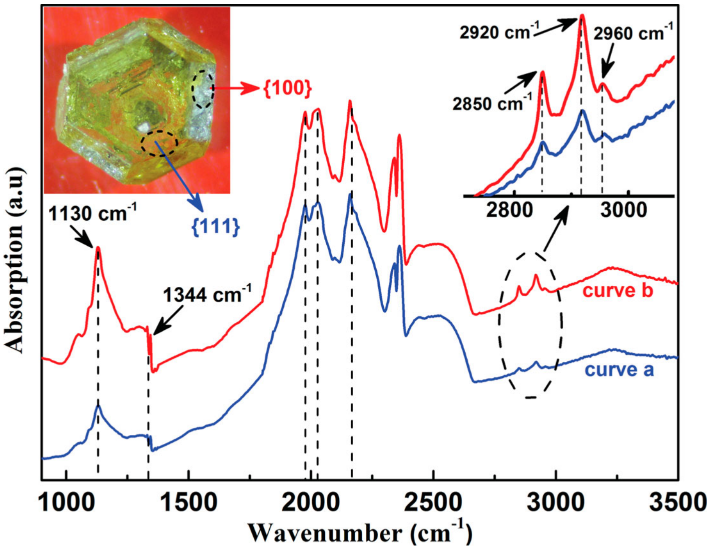

Figure 9. (Colour online) The typical FTIR recorded of the diamond on different crystals faces with 0.3 wt% $C_{10}H_{10}Fe$ addition in the Fe–Ni–C system by TGM: (a) {111} crystal face and (b) {100} crystal face.

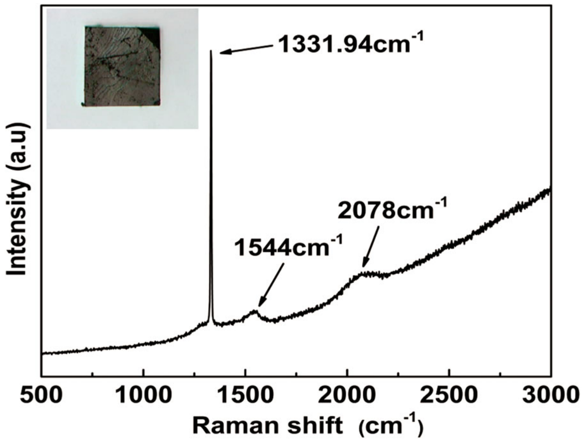

Figure 10. The typical Raman spectra of a sample prepared from a cubic diamond crystal (Run N-5). The inset image lying at top left corners is the corresponding optical image of the diamond sample.

diamond is black. Considering the result of IR absorption, we can infer that this band shift is probably due to the doping of hydrogen atoms in the graphite network.

4. Conclusion

In this work, the effect of hydrogen doping in diamond was investigated in the Fe–Ni–C system by added ideal hydrogen source $C_{10}H_{10}Fe$ under HPHT. The results show that high temperature is a key factor for synthesizing high-quality hydrogen-doped diamond. The presence of hydrogen will greatly degrade the surface quality of diamond crystal, especially the {100} faces. Under low-temperature condition, the nitrogen cooperated with hydrogen atoms more easily enter into the diamond crystal lattice from the {100} surface.

Acknowledgements

The authors thank Dr Yuewen Zhang and Dr Zhuangfei Zhang for their assistance in the course of this study.

Disclosure statement

No potential conflict of interest was reported by the authors.

Funding

This work was supported by the National Natural Science Foundation of China under Grant [number 51172089], Grant [number 11504267] and the Foundation of Guizhou Province Education Department under Grant [number KY [2013]183].

References

[1] Ohashi K, Rosskopf T, Watanabe H, et al. Negatively charged nitrogen-vacancy centers in a 5 nm thin ^{12}C diamond film. Nano Lett. 2013;13:4733–4738.

[2] Burek MJ, Chu YW, Liddy MSZ, et al. High quality-factor optical nanocavities in bulk single-crystal diamond. Nature Communications. 2014;5:5718.

[3] Yoneda A, Xie LJ, Tsujino N, et al. Semiconductor diamond heater in the Kawai multianvil apparatus: an innovation to generate the lower mantle geotherm. High Press Res. 2014;34:392–403.

[4] Yu RZ, Ma HA, Liang ZZ, et al. HPHT synthesis of diamond with high concentration nitrogen using powder catalyst with additive $Ba(N_3)_2$. Diam Relat Mater. 2008;17(2):180–184.

[5] Ekimov EA, Ralchenko V, Popovich A. Synthesis of superconducting boron-doped diamond compacts with high elastic moduli and thermal stability. Diam Relat Mater. 2014;50:15–19.

[6] Levent A, Yardım Y, Senturk Z. Electrochemical performance of boron-doped diamond electrode in surfactant-containing media for ambroxol determination. Sensor Actuat B Chem. 2014;203:517–526.

[7] Mavrin BN, Denisov VN, Popova DM, et al. Boron distribution in the subsurface region of heavily doped IIb type diamond. Physics Letters A. 2008;372:3914–3918.

[8] Zhang JQ, Ma HA, Jiang YP, et al. Effects of the additive boron on diamond crystals synthesized in the system of Fe-based alloy and carbon at HPHT. Diam Relat Mater. 2007;16:283–287.

[9] Hoffman A, Foord J. Hydrogen interactions with diamond. Phys Chem Chem Phys. 2011;13:11469–11470.

[10] Michaelson Sh, Akhvlediani R, Hoffman A. Hydrogenation and thermal stability of nano- and microcrystalline diamond films studied by vibrational electron spectroscopy. J Appl Phys. 2008;104:083527.

[11] Larsson K, Lunell S. Stability of halogen-terminated diamond (111) surfaces. J Phys Chem A. 1997;101:76–82.

[12] Schmandt B, Jacobsen SD, Becker TW, et al. Dehydration melting at the top of the lower mantle. Science. 2014;344:1265–1268.

[13] Sobia AR, Cao JQ, Xia HH, et al. Incorporation of hydrogen in diamond thin films. Diam Relat Mater. 2009;18:1247–1252.

[14] Fernandez-Lorenzo C, Araujo D, Martin J, et al. Hydrogen passivation of boron acceptors in as-grown boron-doped CVD diamond epilayers. Diam Relat Mater. 2010;19:904–907.

[15] Barjon J, Habka N, Chevallier J, et al. Hydrogen-induced passivation of boron acceptors in monocrystalline and polycrystalline diamond. Phys Chem Chem Phys. 2011;13:11511–11516.

[16] Azria R, Lafosse A, Amiaud L, et al. Hydrogenated polycrystalline diamond films: elastic and inelastic electron reflectivity. Prog Surf Sci. 2011;86:94–114.

[17] Sun SS, Jia XP, Zhang ZF, et al. HPHT synthesis of boron and nitrogen co-doped strip-shaped diamond using powder catalyst with additive h-BN. J Cryst Growth. 2013;377:22–27.

[18] Li SS, Ma HA, Li XL, et al. Synthesis and characterization of p-type boron-doped IIb diamond large single crystals. Chin Phys B. 2011;20:028103.

[19] Kindlein Jr. W, Livi RP, Balzaretti NM, et al. Effect of hydrogen implantation on the graphite used in high pressure diamond synthesis. Diam Relat Mater. 2000;9:22–25.

[20] Davydov VA, Rakhmanina AV, Agafonov V, et al. Conversion of polycyclic aromatic hydrocarbons to graphite and diamond at high pressures. Carbon. 2004;42:261–269.

[21] Li Y, Jia XP, Hu MH, et al. Growth and annealing study of hydrogen-doped single diamond crystals under high pressure and high temperature. Chin Phys B. 2012;21:058101.

[22] Zhang ZF, Jia XP, Sun SS, et al. Effects of hydrogen impurity on diamond crystal growth process. Int J Refract Met Hard Mater. 2013;38:111–117.

[23] Sun SS, Jia XP, Yan BM, et al. Synthesis and characterization of hydrogen-doped diamond under high pressure and high temperature. Cryst Eng Comm. 2014;16:2290–2297.

[24] Zang CY, Jia XP, Ma HA, et al. Grow large high-quality diamonds with different seed surfaces. Chin Phys Lett. 2006;23:214–216.

[25] Mcnamara KM, Williams BE, Gleason KK, et al. Identification of defects and impurities in chemical-vapor-deposited diamond through infrared spectroscopy. J Appl Phys. 1994;76:2466–2472.

[26] Yan BM, Jia XP, Fang C, et al. The effect of phosphorus and nitrogen co-doped on the synthesis of diamond at high pressure and high temperature. Int J Refract Met Hard Mater. 2016;54:309–314.

[27] Zhang YF, Zang CY, Ma HA, et al. HPHT synthesis of large single crystal diamond doped with high nitrogen concentration. Diam Relat Mater. 2008;17:209–211.

[28] Liang ZZ, Jia XP, Ma HA, et al. Synthesis of HPHT diamond containing high concentrations of nitrogen impurities using NaN_3 as dopant in metal-carbon system. Diam Relat Mater. 2005;14:1932–1935.

[29] Huang GF, Zheng YJ, Peng LZ, et al. Crystallization of HPHT diamond crystals in a floatage system under the influence of nitrogen and hydrogen simultaneously. Cryst Eng Comm. 2015;17:6504–6511.